

Analysis of Composite De-Laval Nozzle Suitable for Rocket Applications

Raviteja Boyanapalli, Raja Sekhara Reddy Vanukuri, Prudhvi Gogineni, Janakinandan Nookala, Goutham Kumar Yarlagadda, Vinay Babu Gada

Abstract: A nozzle is a device designed to control the direction or characteristics of a fluid flow (especially to increase velocity) as it exits (or enters) an enclosed chamber or pipe via an orifice. A nozzle is often a pipe or tube of varying cross sectional area, and it can be used to direct or modify the flow of a fluid (liquid or gas). Nozzles are frequently used to control the rate of flow, speed, direction, mass, shape, and/or the pressure of the stream that emerges from them. A nozzle is a relatively simple device, just a specially shaped tube through which hot gases flow. However, the mathematics, which describes the operation of the nozzle, takes some careful thought. Nozzles come in a variety of shapes and sizes. Simple turbojets, and turboprops, often have a fixed geometry convergent nozzle as shown on the left of the figure. Turbofan engines often employ a co-annular nozzle as shown at the top left. The core flow exits the centre nozzle while the fan flow exits the annular nozzle. Mixing of the two flows provides some thrust enhancement and these nozzles also tend to be quieter than convergent nozzles. Afterburning turbojets and turbofans require a variable geometry convergent-divergent - CD nozzle. In this nozzle, the flow first converges down to the minimum area or throat, then is expanded through the divergent section to the exit at the right. The variable geometry causes these nozzles to be heavier than a fixed geometry nozzle, but variable geometry provides efficient engine operation over a wider airflow range than a simple fixed nozzle. Rocket engines also use nozzles to accelerate hot exhaust to produce thrust. Rocket engines usually have a fixed geometry CD nozzle with a much larger divergent section than is required for a gas turbine. All of the nozzles discussed thus far are round tubes. Recently, however, engineers have been experimenting with nozzles with rectangular exits. This allows the exhaust flow to be easily deflected, or vectored. Changing the direction of the thrust with the nozzle makes the aircraft much more manoeuvrable. Because the nozzle conducts the hot exhaust back to the free stream, there can be serious interactions between the engine exhaust flow and the airflow around the aircraft. On fighter aircraft, in particular, large drag penalties can occur near the nozzle exits. As with the inlet design, the external nozzle configuration is often designed by the airframer and subjected to wind tunnel testing to determine the performance effects on the airframe. The internal nozzle is usually the responsibility of the engine manufacturer.

I. INTRODUCTION

De-Laval nozzle (or convergen - divergent nozzle, CD nozzle or con-di nozzle) is a tube that is pinched in the middle, making a carefully balanced, asymmetric hourglass-shape. It is used to accelerate a hot, pressurized gas passing through it to a supersonic speed, and upon expansion, to shape the exhaust flow so that the heat energy propelling the flow is maximally converted into directed kinetic energy. Because of this, the nozzle is widely used in some types of steam turbines, it is an essential part of the modern rocket engine, and it also sees use in supersonic jet engines.

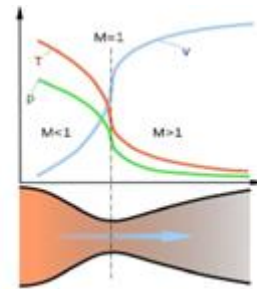


Fig-1: Diagram of a De-Laval nozzle, showing approximate flow velocity(v), together with the effect on temperature (t) and pressure (p)

The nozzle was developed by Swedish inventor Gustaf de Laval in 1888 for use on a steam turbine. This principle was first used in a rocket engine by Robert Goddard. Very nearly all modern rocket engines that employ hot gas combustion use de Laval nozzles.

II. WORKING

De naval nozzles work based on Bernoulli's principle of fluid dynamics. This also allows calculation of mass flow rate of propellant.

$$P_a + \frac{1}{2} \rho V_a^2 + \rho g H_a = P_b + \frac{1}{2} \rho V_b^2 + \rho g H_b$$

- Where,
- a - first point along the pipe line
 - b - second point along the pipe line
 - P - static pressure in N/m^2
 - ρ - density in kg/m^3
 - V - velocity in m/s
 - g - acceleration due to gravity in m/s^2
 - H - static head in m



Manuscript published on 30 April 2013.

*Correspondence Author(s)

Mr. Raviteja Boyanapalli, Department of Mechanical Engineering, KL University, Vijayawada, India

Mr. Raja Sekhara, Department of Mechanical Engineering, KL University, Vijayawada, India

Mr. Prudhvi Gogineni, Department of Mechanical Engineering, KL University, Vijayawada, India

Mr. Goutham Kumar Yarlagadda, Department of Mechanical Engineering, KL University, Vijayawada, India

Mr. Janakinandan Nookala, Department of Mechanical Engineering, KL University, Vijayawada, India

Mr. Vinay Babu Gada, Department of Mechanical Engineering, KL University, Vijayawada, India.

© The Authors. Published by Blue Eyes Intelligence Engineering and Sciences Publication (BEIESP). This is an open access article under the CC-BY-NC-ND license <http://creativecommons.org/licenses/by-nc-nd/4.0/>

This is based on three laws of conservation viz., mass, momentum and energy. Since momentum is constant, if the mass of rocket decreases due to the loss of fuel, the rocket velocity increases. Convergent end of the nozzle is wide, narrow and accelerates subsonic flows. Divergent end of the nozzle tends to variable density; sonic/supersonic flows are accelerated. Major design criterion is the expansion ratio i.e., the ratio of exit area to that of the throat area. If the pressure ratio is high enough, flow will reach sonic, reaching the state of “*choking*”, however further increase does not raise the throat mach the number.

A. Operation

Its operation relies on the different properties of gases flowing at subsonic and supersonic speeds. The speed of a subsonic flow of gas will increase if the pipe carrying it narrows because the mass flow rate is constant. The gas flow through a de Laval (gas entropy is nearly constant). At subsonic compressible; sound, a small pressure wave, will propagate through it. At the “throat”, where the cross sectional area is a minimum, the gas velocity locally becomes sonic (Mach number = 1.0), a condition called choked flow. As the nozzle cross sectional area increases the gas begins to expand and the gas flow increases to supersonic velocities where a sound wave will not propagate backwards through the gas as viewed in the frame of reference of the nozzle (Mach number > 1.0).

B. Conditions for Operation

A de Laval nozzle will only choke at the throat if the pressure and mass flow through the nozzle is sufficient to reach sonic speeds, otherwise no supersonic flow is achieved and it will act as a venturi-tube; this requires the entry pressure to the nozzle to be significantly above ambient at all times (equivalently, the stagnation pressure of the jet must be above ambient). In addition, the pressure of the gas at the exit of the expansion portion of the exhaust of a nozzle must not be too low. Because pressure cannot travel upstream through the supersonic flow, the exit pressure can be significantly below ambient pressure it exhausts into, but if it is too far below ambient, then the flow will cease to be supersonic, or the flow will separate within the expansion portion of the nozzle, forming an unstable jet that may ‘flop’ around within the nozzle, possibly damaging it.

In practice ambient pressure must be no higher than roughly 2-3 times the pressure in the supersonic gas at the exit for supersonic flow to leave the nozzle.

C. Flow Analysis in De-Laval Nozzles

The analysis of gas flow through de Laval nozzles involves a number of concepts and assumptions:

1. For simplicity, the gas is assumed to be an ideal gas.
2. For simplicity, the gas is assumed to be an ideal gas.
3. The gas flow is isentropic (i.e., at constant entropy). As a result the flow is reversible (frictionless and no dissipative losses), and adiabatic (i.e., there is no heat gained or lost).
4. The gas flow is constant (i.e., steady) during the period of the propellant burn.

5. The gas flow is along a straight line from gas inlet to exhaust gas exit (i.e., along the nozzle’s axis of symmetry)
6. The gas flow behavior is compressible since the flow is at very high velocities.

D. Exhaust Gas Velocity

As the gas enters a nozzle, it is travelling at subsonic velocities. As the throat contracts down the gas is forced to accelerate until at the nozzle throat, where the cross-sectional area is the smallest, the linear velocity becomes sonic. From the throat the cross-sectional area then increases, the gas expands and the linear velocity becomes progressively more supersonic.

The linear velocity of the exiting exhaust gases can be calculated using the following equation:

$$V_e = \sqrt{\frac{T R}{M} \cdot \frac{2 k}{k-1} \cdot \left[1 - (P_e/P)^{(k-1)/k} \right]}$$

where:

V_e = Exhaust velocity at nozzle exit, m/s

T = absolute temperature of inlet gas, K

R = Universal gas law constant = 8314.5 J/(kmol·K)

M = the gas molecular mass, kg/kmol (also called molecular weight) $k = cp/cv$ = isentropic expansion factor

cp = specific heat of the gas at constant pressure

cv = specific heat of the gas at constant volume

P_e = absolute pressure of exhaust gas at nozzle exit, kPa

P = absolute pressure of inlet gas, kPa

Some typical values of the exhaust gas velocity V_e for rocket engines burning various propellants are:

- 1700 to 2900 m/s (3,800 to 6,500 mph) for liquid monopropellants.
- 2900 to 4500 m/s (6,500 to 10,100 mph) for liquid bipropellants.
- 100 to 3200 m/s (4,700 to 7,200 mph) for solid propellants.

As a note of interest, V_e is sometimes referred to as the ideal exhaust gas velocity because it based on the assumption that the exhaust gas behaves as an ideal gas.

As an example calculation using the above equation, assume that the propellant combustion gases are: at an absolute pressure entering the nozzle of $P = 7.0$ MPa and exit the rocket exhaust at an absolute pressure of $P_e = 0.1$ MPa; at an absolute temperature of $T = 3500$ K; with an isentropic expansion factor of $k = 1.22$ and a molar mass of $M = 22$ kg/kmol. Using those values in the above equation yields an exhaust velocity $V_e = 2802$ m/s or 2.80 km/s which is consistent with above typical values.

The technical literature can be very confusing because many authors fail to explain whether they are using the universal gas law constant R which applies to any ideal gas or whether they are using the gas law constant Rs which only applies to a specific individual gas. The relationship between the two constants is $R_s = R/M$.

E. Working Of Rocket Engine

Rocket engines may either work with solid or liquid propellants or as a combination of both, hybrid propulsion systems, such as the one for the Spaceship – 1 project. Liquid rocket engines can be subdivided into mono-propellant or bi-propellant systems. Mono-propellant engines operate either as a simple cold gas system or apply a catalyst for an exothermal decomposition of the propellant, such as hydrazine (N2H4) or laughing gas (N2O). Generally these type of engines are only in use for low thrust satellite propulsion systems.

Typical bi-propellant engines use either earth storable propellants, generally combinations of nitric acid or its anhydride with derivates of hydrazine, i.e. asymmetric dimethyl hydrazine (UDMH) or mono-methyl-hydrazine (MMH), mixtures of storable and cryogenic propellants, liquid oxygen and kerosene or fully cryogenic, liquid oxygen and liquid hydrogen.

Although rocket engines show large differences depending on mission profile and staging of the launcher it is possible useful to separate them in four major classes. Booster, main stage and upper stage engines and satellite propulsion and attitude control systems. Rocket engines are energy conversions systems with a heat release in the combustion chamber which exceed by far typical values of nuclear power plants (~ 3-4 GW). While solid rocket engines may even reach power levels of more than 30 GW, the most powerful liquid rocket engines have peak power values of up to 20 GW but the majority works with values of less than 10 GW.

Obviously such power levels are only possible with high combustion chamber pressures and even higher propellant mass flow rates which may exceed 1000 kg/s.

III.NOZZLE INSERT MATERIALS

NOZZLE MATERIALS

Class	Material	Fabrication
Refractory Metals	Molybdenum Tungsten Tungsten Tungsten Tungsten,75% dense Tungsten, 65% dense	Arc cast Arc cast Arc cast Cold pressed, sintered & forged Cold pressed and sintered Cold pressed and sintered
Refractory compounds	4 Parts tantalum carbide and 1 part zirconium carbide with graphite 4 Parts tantalum carbide and 1 part hafnium carbide with graphite Columbium carbide with graphite 8 Parts tantalum carbide and 1 part zirconium carbide with graphite Tantalum carbide with graphite Tantalum carbide with tungsten Columbium carbide with tungsten Columbium carbide with tungsten and silver infiltrant a LT1BbLT2 Silicon nitride	Hot pressed Cold pressed and sintered Cold pressed and sintered Cold pressed, sintered and infiltrated Slip cast and sintered Slip cast and sintered Slip cast and sintered
Graphite	ZT graphite Speer 3499 graphite ATJ graphite	Molded and recrystallized Molded Molded
Reinforced plastics	Phenolic refrasil (40 percent resin) Phenolic refrasil (20 percent resin) Phenolic with graphite Phenolic with nylon	Molded

aLTIB: 59 chromium, 19 aluminum oxide, 20 molybdenum, 2titanium oxide.

bLT2: 60 tungsten, 25 chromium, 15 aluminium oxide.

The general classes of materials investigated were refractory metals, refractory compounds, graphites, and reinforced-plastic materials. In most cases nozzle insert materials were obtained from commercial sources in semi finished form, and final machining was performed at the Lewis Research Centre.

The reinforced-plastic nozzles were obtained from commercial sources completely finished. The graphite nozzles were machined so that the axial direction was parallel to the direction in which the graphites were pressed during moulding.

The refractory – metal - carbide - graphite nozzle compositions varied radially with essentially pure carbide at the inner diameter and increasing amounts of graphite content toward the outer diameter. The refractory metal carbide- tungsten nozzles were formed by a proprietary carbon exchange process in which, for example, a mixture of tungsten carbide and tantalum metal was transformed during processing to a mixture of tantalum carbide and tungsten metal.

A. Nozzle Erosion

Erosion mechanisms fall into three distinct categories: melting or sublimation, oxidation, and mechanical abrasion. In general, the erosion characteristics of materials when exposed to the combustion gases of various propellants can be related to material properties and thermal and chemical environments. These relations are described for the various types of materials in the following sections.

B. Refractory Metals

Overall, the fully dense refractory metals were the most erosion resistant group of materials. Molybdenum did not erode in the two lower temperature propellant environments, but it eroded catastrophically with the highest temperature propellant. In general, the high-density (arc-cast, sintered, and forged) tungsten nozzles performed with only slight to moderate erosion with all three propellants. The one nozzle that experienced severe erosion (commercial arc-cast tungsten) showed grain separation during machining. The lower density powder-metallurgy tungsten nozzles eroded catastrophically in the two more oxidizing propellants. However, no erosion occurred with the least oxidizing, intermediate-temperature propellant. The failure mechanisms involved with these materials differed. Molybdenum did not erode with the most oxidizing propellant or with the relatively abrasive intermediate temperature aluminized propellant. This suggests that molybdenum was not particularly susceptible to oxidation or abrasion except at the highest flame temperature. The HDBM propellant flame temperature is approximately 1700' F higher than the melting point of molybdenum. It is probable that the catastrophic erosion observed for this material was due to melting and oxidation.



Although data were not obtained for a molybdenum nozzle with the HDBM propellant, temperature data obtained with tungsten and ZT graphite nozzles when exposed to the HDBM propellant indicate that the nozzle surface temperature of molybdenum would be expected to approach the melting point with this propellant.

Also, the fact that substantial erosion occurred very early in the firing, probably before the melting point of molybdenum had been reached, suggests that oxidation occurred. Finally, X-ray diffraction data of scrapings taken from the nozzle after firing indicated the presence of molybdenum oxide.

In the tests of the high-density tungsten nozzles, measurable erosion was observed only with the Arcite 368 propellant (table III). Since this propellant provided the lowest temperature, most oxidizing, and least abrasive environment, it is most likely that oxidation was the failure mechanism in this case.

The low-density tungsten nozzles failed catastrophically with both Arcite 368 and HDBM propellants and did not erode with the Arcite 373 propellant. These results also suggest that oxidation was the primary mechanism, but deterioration was probably aggravated by mechanical abrasion of these relatively weak porous structures.

C. Refractory Compounds

By definition the refractory compounds considered in this project include the refractory- metal-carbide - graphite combinations, refractory metal- carbide - tungsten materials, metal-impregnated refractory compounds (including cermets), and a ceramic (silicon nitride). The refractory-metal-carbide - graphite materials showed essentially no erosion with the Arcite 373 propellant, but severe or catastrophic erosion occurred with the Arcite 368 propellant except for the tantalum carbide - graphite nozzle, which showed only slight erosion. The performance of these materials with the highest temperature HDBM propellant was intermediate to that obtained with the other propellants. These results suggest that erosion resulted primarily from oxidation, since erosion increased with increasing severity of oxidizing environment.

The refractory-metal-carbide - tungsten nozzles (except for the silver infiltrated nozzle) showed outstanding performance in resisting erosion, comparable to that of the best refractory-metal nozzle (slight to moderate erosion with all propellants). However, thermal-stress cracking was encountered. Such erosion as did occur was probably due to oxidation since the greatest erosion occurred with the most oxidizing propellant.

The silver infiltrated columbium carbide - tungsten material eroded only slightly with the HDBM propellant but eroded catastrophically with the more oxidizing Arcite 368. It is possible that the greater surface area exposed as the silver was melted from the porous columbium carbide - tungsten skeleton contributed to making the nozzle more subject to

oxidation than the fully densified columbium carbide - tungsten. While a nozzle of this material was not available for firing with the 373 propellant, erosion would not be expected to occur with this, the least oxidizing propellant.

The cermets and the silicon nitride nozzles eroded only slightly with the most oxidizing propellant, but catastrophic erosion occurred with the least oxidizing, intermediate temperature propellant. The catastrophic erosion of these materials was attributed to melting or sublimation.

Melting of LT1B and LT2 and sublimation of silicon nitride occur at temperatures ranging from 3100' to 3500' F.

Estimates based on material properties and measured nozzle temperatures of other materials indicate that the nozzle surface temperature of the two cermet and the silicon nitride nozzles were probably above the melting or sublimation temperature when exposed to the 5600' F Arcite 373 propellant.

Graphites

Graphites in general showed relatively poor erosion resistance in comparison with the refractory metals. Erosion varied from moderate to catastrophic for the two more oxidizing propellants, while essentially no erosion was observed with the least oxidizing propellant. Thus, it is evident that oxidation was the major failure mechanism.

It may also be inferred from the results that mechanical abrasion was a contributing failure mechanism. Of the two propellants with which severe erosion was observed, HDBM and Arcite 368, the greater degree of erosion occurred with the aluminum-bearing HDBM propellant. Another indication that mechanical abrasion was a contributing factor is the fact that the higher density, higher strength ZT graphite was substantially more resistant to erosion with the aluminium-bearing HDBM propellant than the conventional moulded ATJ graphite.

If mechanical abrasion contributed to failure, the erosion rate would be expected to diminish with reduced chamber pressure. That the erosion rate was diminished for two of the graphite materials is evident from the pressure traces in which the pressure regression is relatively flat in the lower pressure region as compared to the initial high pressure operation.

This may be seen quantitatively by comparison of the erosion rate data for the same portions of the pressure regression. For example, the high-pressure erosion rate of the ATJ nozzle with the HDBM propellant was relatively high, 7.8 mils per second. Calculation of the erosion rate for the remaining pressure regression indicates a much lower value of 0.8 mil per second.

Fibre-reinforced plastics

Severe or catastrophic erosion occurred by ablation with all fiber-reinforced plastic nozzles tested. The severity of erosion increased with increased flame temperature. For example, total erosion of the 40 percent resin phenolic-refrasil nozzle increased from approximately 26 to 142 mils when the nozzle was tested with Arcite 368 and 373 propellants, respectively. Since melting and volatilization of plastic materials normally occurs in the ablative process, the increased flame temperature of the 373 propellant would be expected to increase erosion.



In addition, the ablative effectiveness of the refrasil-reinforced nozzles was probably reduced by reaction (fluxing) between the silica in the nozzle and the aluminium oxide in the Arcite 373 propellant combustion products.

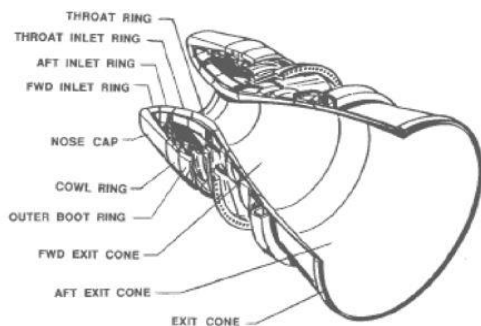
More specifically, this lower effectiveness could be attributed to the lower melting point of the glass formed, and the attendant reduction in viscosity would allow the molten glass to be more readily swept from the nozzle surface. As in the case of the graphites, the fiber-reinforced plastic nozzles showed a lower erosion rate with lower pressure operation as compared with that at high pressure.

In this case with the Arcite 368 propellant the high-pressure erosion rate was 3.6 mils per second as compared with 0.39 mil per second for the remaining pressure regression. The generally poor performance demonstrated by these materials at these operating pressures precluded additional firings with the higher temperature propellants.

D. Thermal -Stress Cracking

Of all of the materials investigated, only the refractory compounds and the lower density, porous-tungsten nozzles developed thermal-stress cracks. In all instances, however, the nozzles remained in place, and no sudden decreases in chamber pressure were noted. Some nozzles were cracked extensively both radially and circumferentially so that nozzles separated into several pieces on removal from the retainer. The silicon nitride, cermet, and refractory-metal-carbide - graphite nozzles cracked extensively. The refractory-metal-carbide - tungsten nozzles cracked less severely than the carbide-graphite type; in some cases only a single fracture occurred.

It should be emphasized that there is an important size factor which must be taken into consideration in extrapolating the thermal-stress performance of nozzles in small scale tests to full-size applications. The effect of nozzle size on thermal stresses is complex and cannot be determined readily. Comparisons based on simplified models have indicated that the thermal stresses induced in the small nozzles of this investigation appear to be lower than those that would occur in a typical large nozzle. Accordingly, nozzle materials that cracked extensively in this investigation would also not be suitable for most large-scale applications. Materials that cracked only slightly in this investigation would be expected to crack more extensively in many large-scale applications.



Solid Rocket Motor Nozzle

Fig.-2: Solid Rocket Motor Nozzle

IV. ANALYSIS OF MATERIALS

The range of conditions considered in this investigation necessarily places certain limitations on the interpretation of the relative performance of the various materials investigated. It should be emphasized that, under other conditions of exposure, the relative rating of nozzle materials could be considerably different from that indicated in the present investigation. The major factors influencing the results are flame temperature, chamber pressure, chemical reactivity of the combustion gases, and nozzle size.

Although high-density tungsten demonstrated overall superiority in resisting erosion and thermal-stress cracking in the tests described in this report, it is expected that use of propellants with appreciably higher flame temperatures would preclude the use of tungsten. Instead, it is likely that only materials such as the refractory-metal carbides would have the potential for application in uncooled nozzles if propellants with flame temperatures of the order of 7000° F and above are successfully developed. Of course, the potential of the carbide nozzle materials would be improved if the chemical reactivity of the higher temperature propellant combustion products were low and if the thermal stress problem could be overcome, perhaps by improved design.

Just as the use of higher temperatures would affect the relative merits of nozzle materials, so would the use of very low chamber pressures. It was noted in the results of this investigation that both the graphite and the fibre-reinforced phenolic materials demonstrated improved erosion resistance at lower chamber pressures. Hence, at very low pressures, such as 100 pounds per square inch, these materials may be preferable to refractory metals, especially where weight and fabricability are important factors.

The relative merit of fibre-reinforced plastic nozzles also may be improved in applications to very large rocket nozzles. Rocket motors are now under development in which the nozzle throat diameter may be well over 6 feet. In nozzles of this size, removal of ablative material from the surface at rates of several mils per second is unimportant since the nozzle area and thrust would be essentially unaffected even for firing durations of several minutes.

Finally, it should be noted that, in areas other than the nozzle throat, such as nozzle entrance and exit cones, where material loss can better be tolerated, fiber reinforced plastics as well as graphite have found widespread use. Of course, in these areas environmental conditions are less severe, and thus material loss would tend to be reduced. An investigation was conducted to determine the performance of uncooled rocket nozzle insert materials in small-scale solid-propellant rocket engines. The materials investigated include refractory metals, refractory-metal carbides, graphites, ceramics, cermets, and fiber-reinforced plastics. Propellants with flame temperatures of 4700°, 5600°, and 6400° F were used. These varied widely in oxidation characteristics.

The 4700° F propellant, which was not aluminized, provided the most oxidizing and least abrasive environment, whereas the 5600° F propellant provided the least oxidizing environment. Both the 5600° F and 6400° F propellants contained aluminum and thus provided very abrasive exhaust products. The test engines were designed to provide a chamber pressure of 1000 pounds per square inch and a firing duration of 30 seconds with a nozzle throat diameter of 0.289 inch. The following results were obtained:

1. No one material performed best with all three propellants. Failure by erosion or cracking occurred with each material with at least one propellant. However, certain classes of materials demonstrated superior performance under specific operating conditions.
2. The fully densified refractory-metal nozzles generally were more resistant to erosion and cracking than the other materials. In those cases where erosion occurred, the refractory metals as a group tended to fail by chemical reaction or by a combination of chemical reaction and mechanical abrasion. The latter failure mechanism occurred with lower density tungsten nozzles fabricated by powder-metallurgy techniques. The relatively slight erosion that occurred with the high-density tungsten (i. e., arc-cast or sintered and forged) nozzles was attributed to oxidation. Thermal-stress cracks were noted in a few low-density tungsten nozzles. Arc-cast molybdenum nozzles showed no evidence of erosion with the two lower temperature propellants. However, severe erosion, attributed to melting and oxidation, occurred with the highest temperature propellant.
3. The graphite nozzles were essentially not eroded by the least oxidizing (5600° F) propellant. However, when exposed to the other two propellants, they were eroded by a combination of chemical reaction and mechanical abrasion. As a group, these nozzles generally eroded more extensively than the refractory metals, but none failed by thermal cracking. The higher density recrystallized graphite performed appreciably better than conventional molded types.
4. All the refractory-metal carbide nozzles failed by thermal-stress cracking. In addition, most of these nozzles were eroded by chemical reaction where the propellant environment tended to promote this failure mechanism. Several of the carbide nozzles showed outstanding erosion resistance with all three propellants, comparable to the best refractory-metal nozzle. These materials, because of their high melting points, may afford a potential advantage for application at flame temperatures above those used in this investigation.
5. The cermet and silicon nitride materials performed well insofar as resistance to erosion was concerned with the lowest temperature propellant despite the oxidizing environment, but the low melting or sublimation point of the cermet and silicon nitride materials places a definite limit on the flame temperatures that they can withstand. In addition, thermal-stress cracking was observed. Exposure to the

intermediate temperature propellant resulted in severe erosion caused by melting or sublimation.

6. Fiber-reinforced plastic nozzles as a class were the least erosion-resistant materials. They eroded catastrophically by ablation with the two lower temperature propellants and were therefore not tested with the 6400° F propellant.

A. Composite De-Laval Nozzle

Light weight (small fibre diameter) high-purity silica reinforced plastics are being used extensively for ablative cooling applications in both liquid and solid rocket-engine thrust chambers. System design simplicity together versatility of fabrication of chambers has definite advantages contributing to overall reliability. However, the primary problem requiring attention is excessive throat erosion or sacrificial mass loss which is responsible for engine-performance losses during the operating life of the thrust chamber. Since the specific-impulse losses are inversely proportional to engine-throat size at a constant erosion rate, the engine-performance losses are most severe in small engines. As engines increase in size, structural requirements also increase; thus, in addition to a high erosion resistance, a large ablative engine should also possess high char strength at low char rates to minimize weight requirements. Prior to study of optimization of ablative composites, a class of ablative materials must be chosen which will exhibit reasonable ablative characteristics in a given combustion environment. Generally, for any given class of ablative materials, the radial erosion rate is primarily a function of the surface temperature and the oxidation or reduction potential in the boundary layer. Two recently completed investigations were conducted to evaluate several types of commercially available ablative materials of nozzle section of a hydrogen-oxygen rocket engine and of a storable-propellant (nitrogen tetroxide N₂O₄ and a 50-50 blend of unsymmetrical dimethyl hydrazine UDMH with hydrazine N₂H₄) engine. The ablative materials in both investigations were tested at a nominal chamber pressure and throat diameter of 100psia (689kN/m²) and 1.20 inches (3.04 cm), respectively. Similar results were obtained with respect to the relative order of throat-erosion resistance for the various material classes. The high-purity-silica reinforced materials had, as a class, erosion resistance superior to all material classes tested. The primary objective of the present investigation was to evaluate the erosion resistance of several high-purity-silica reinforced ablative materials as nozzle sections of a 7.8 inch diameter throat (nominal Apollo sizes), storable-propellant rocket engine. A secondary objective was to perform a preliminary study of the effects on erosion of some major material and processing variables including resin content and cloth-fibre diameter. The nominal engine conditions included an oxidant to fuel ratio of 2.00, constant chamber pressure of 100psia (689 kN/m²), and an initial throat diameter of 7.82inches (19.8 cm).



All testing was conducted at an ambient pressure of 1.60psia (11.05 kN/m²). Results are presented for 11 high-purity–silica reinforced ablative materials in terms of nozzle–throat dimensional change as a function of run time. Char thickness, if it is available, is presented as percent char, from original thickness, to the outer asbestos insulation.

B. Ablative Material Samples

No attempt was made to correlate results with a particular material supplier as samples were chosen for their basic constituents only without regard to the source.

The ablative materials samples have been evaluated in the present investigation are listed in table.1. The samples have been numbered in the order presented in the table, and this number is used here in to identify the samples. in addition , the table lists all pertinent information which is necessary to adequately describe each sample. four nozzles with cloth layed up in a rosette, six nozzles with fibres oriented 90° to the centre-line, and one nozzle with material of 1/2-inch chopped square(1.27-cm squares) were tested. a rosette–type fibre orientation is layed up in plies which run longitudinally, at a given helix angle, in contrast to fabric layed up circumferentially with respect to the nozzle centreline. Figure shows nozzles with a typical rosette layup, a standard fibre-orientation angle of 90 degrees ,and chopped material of 1/2-inch squares. Two of the 90 degrees fibre orientation nozzles (6&7) were hand impregnated by the supplier after removal of all the fill fibres. All the remaining fibres were radially oriented with respect to nozzle centreline .The phenolic resin used in all samples conformed to the requirements of specification MIL-R-9299. Samples 3 was intended to be a direct comparison sample-2 to assess the effect modified chromium salt additive to an 0.008in and a 0.015 inch fibre diameter, respectively.However, the chromium salts in the small fibre-diameter material were difficult to convert in to modified form, and, therefore a proprietaryresin was used as a substitute in an attempt to duplicate this modification during the firing . The rosette nozzles were layed up in a female tool and hydroclaved at 1000psi(6894 kn/metre square) pressure, and the remaining nozzles were compression molded in matched metal dies at 3000psia(20660kn/metre square) pressure.

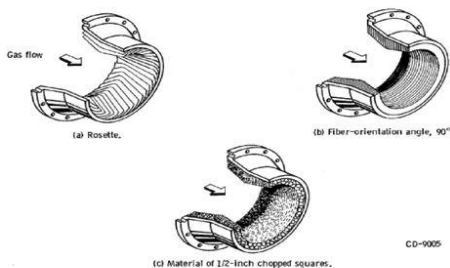


Fig.-3: Nozzle Configuration

The experiment test runs conducted in the altitude facility shown in figure2. A view of the test chamber area is shown in figure3. A test engine mounted to the thrust stand and the entrance to the exhaust collector can be seen

C. Facility

The fuel (50-50 blend of UDMH and hydrazine) tank had a capacity of 560 gallons (2.12m³) while the oxidant (n2o4) tank capacity is 707 gallons(2.67m³). a capability for over 400 seconds continuous operation was therefore possible at a chamber pressure of 1000psia (689 kn/metre square), an oxidant -to-fuel ratio of 2.0, and a constant throat diameter of 7.82 inches (19.8 cm).

TABLE 1 - ABLATIVE-MATERIAL SAMPLES

Sample	High-silica reinforcement			Cloth		Additive		Orientation	Resin		Binder		Molding conditions		
	Fiber diameter, in.	Weight, percent	Type	Weight, percent	Type	Weight, percent	Type		Weight, percent	Type	Temperature, °C	Pressure, psia	Time, hr		
1	0.015	71	Chromium salt	3	Phenolic	27	Phenolic	Rosette, 30°	Phenolic	27	Polymide	300	1000	4	
2	0.015	71	Chromium salt	3	Phenolic	27	Phenolic	Rosette, 30°	Phenolic	27	Polymide	300	1000	4	
3	0.008	71	Chromium salt	3	Phenolic	27	Phenolic	Rosette, 30°	Phenolic	27	Proprietary modification	325	3000	3	
4	0.008	73	None	3	Phenolic	35	Phenolic	Rosette, 30°	Phenolic	35	Proprietary modification	325	3000	3	
5	0.008	77	None	3	Phenolic	30	Phenolic	Rosette, 30°	Phenolic	30	Proprietary modification	325	3000	3	
6	0.008 (modified form)	78	None	3	Phenolic	30	Phenolic	Rosette, 30°	Phenolic	30	Proprietary modification	325	3000	3	
7	0.008 (modified form)	65	None	3	Phenolic	30	Phenolic	Rosette, 30°	Phenolic	30	Proprietary modification	325	3000	3	
8	0.015	60	None	3	Phenolic	30	Phenolic	1/2-inch squares	Phenolic	30	Elastomer	325	3000	3	
9	0.015	62	None	3	Phenolic	30	Phenolic	1/2-inch squares	Phenolic	30	Phenolic powder	325	3000	3	
10	0.015	62	None	3	Phenolic	30	Phenolic	1/2-inch squares	Phenolic	30	Phenolic powder	325	3000	3	
11	0.015	62	None	3	Phenolic	30	Phenolic	1/2-inch squares	Phenolic	30	Phenolic powder	325	3000	3	

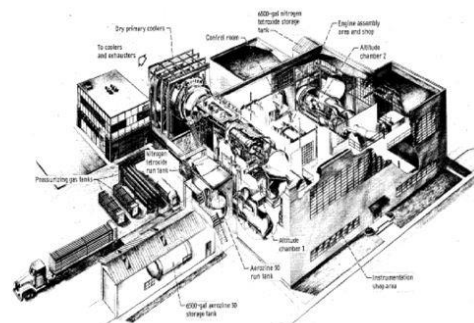


Fig.-4: Nozzle Engine

V. TESTING PROCEDURE

The operation of the instrumentation was verified, and the engine assembly pressure checked prior to each run. The propellant tanks were loaded and pressurized with nitrogen gas. The closed-loop controller was set to maintain a constant chamber pressure of 100 psia (689 kN/m²) and an oxidant-to-fuel ratio of 2.0 during the firing duration. Changes in chamber pressure due to throat area change were compensated by corresponding changes in the propellant-flow rate. The altitude chamber was evacuated to approximately 1.60 psia (11.05 kN/m²) pressure, and the high-pressure pumps were activated to supply cooling water to the chamber. A sequence timer automatically activated appropriate valves, data acquisition equipment, and propellant -line purges for each run. An oscilloscope was used to monitor possible combustion instability (determined from a water-cooled flush-mount pressure transducer located on the inside diameter of the combustion chamber). An abort switch was normally activated 1 or 2 seconds after detection of any high-frequency instability (usually 2200 cycles per second (2200Hz), 1st tangential mode). On these few occasions, the restarted engine was free of high-frequency instability. All the ablative nozzles were subjected to a single continuous firing duration of at least 250 seconds. Nozzles 4, 5, 7, 8, and 10 were arbitrarily run for longer continuous durations to check on gouging potential and to determine if the steady-state erosion rate was appreciably changed when char to the insulation was evident. The throat diameter of each ablative nozzles was measured before and after running, and each was subsequently sectioned for visual inspection and photographed. Char-thickness measurements were obtained for nine of the nozzles tested.

VI. COMPARISON OF ALL NOZZLES TESTED:

A summary of the test results presented in table-II which lists the ablative nozzles in order of decreasing erosion resistance nozzle(4) was run for 325 seconds, four nozzles(5,7,8 and 10) were run for 350 seconds, and the six remaining nozzles run for 250 seconds for direct comparison, the overall erosion rates (change in radius/run time) were calculated for the initial 250 seconds. data concerning char are also included and are presented as the present char to the asbestos insulation, as a function of the original wall thickness, after the firing has been completed, char was measured at the throat plane only since some gouging did occur, and the char formation is meant to be an estimate for comparison only. Typical charts are presented in figures. Nozzle 4 had less than one-half the erosion rate after 250 seconds of firing that nozzle 9 exhibited. However, both experienced the same percent char, although nozzle 4 runs 75 seconds longer. For a constant erosion rate, a low char rate would require less insulation; thereby, a weight saving would be effected. The rosette layup appeared to decrease the char rate while it maintained a low erosion rate.

VII. RESULTS AND DISCUSSIONS:

The variation of erosion rate with small changes in injector performance is very significant, and therefore, it was essential to maintain constant characteristic velocity efficient throughout the program of equal importance was the relatively high value obtained (0.970) as it is possible not to experience dimensional ablation if the injector efficiency is too low.

Checks on the characteristic velocity efficiency were made using the heat-sink nozzle after every second or third ablative - material nozzle run. the characteristic velocity efficiency calculated from thrust measurements was maintained at 0.970 throughout the entire test program, indicating no deterioration of the injector.

D. Throat Erosion of Ablative Material Nozzle Sections

When the throat radius change was plotted against run time, atypical curve corresponding to the one produced in figure 8 was obtained. The typical nozzle erosion curve can be divided into three major portions. The first section of the curve, the area under the zero erosion line, is defined as "reduced effective throat area." This decrease in the effective throat area is caused by resin decomposition and subsequent discharge of the pyrolysis products into the boundary layer together with material swelling and expansion effects which occur throughout the entire firing but are particularly pronounced during the initial firing phase. The second section of the curve represents steady state erosion, and the last section shows accelerated erosion near the end of the run, indicating complete char to the insulation (resin depletion) and /or fibre deterioration which results in rapid char-layer removal.

In an effort to gain an understanding of the cause-effect relation of the various material and processing techniques involved, individual nozzles were compared to each other with respect to a major variable and are discussed in the following sections.

Although only one nozzle of each type was tested and the statically confidence level is not high, the discussion is meant to serve as a possible guide to future studies, Fabric-Fibre Diameter Nozzles 5 and 8, presented in figure 9, compare the erosion resistance of two basic fabric weaves.

Nozzle 5 was made from a high-silica cloth in which the individual fibre strands or filament bundles are approximately one-half the diameter (0.008in.(0.203mm) compared with 0.015in.(0.381mm) of the fibre strands used to fabricate nozzle 8. The erosion resistance of the smaller - diameter fibre material was slightly superior to the larger-diameter fibre material, especially near the end of the firing.

The superior erosion resistance of the smaller -diameter fibre over the larger diameter fibre possibly may be explained in terms of fibre surface area. The smaller individual fibre diameters whirr result in a nozzle in which the reinforcement has a larger total surface area. The increased surface area promotes easier penetration of the individual fibers by the impregnating resin, which in turn effects the homogeneity and tends to increase the density of the resultant char and to improve the shear force resistance.

Silica Fabric And Material of ½ inch Chopped Squares - Nozzles 10 and 11, presented in figure 10, are a comparison of the erosion resistance between a silica-powder-filled phenolic system employing a fabric layup 90 degree to centreline and a chopped moulding compound of ½-inch squares randomly oriented. Nozzle 10, the fabric layup, appeared to be slightly superior to the chopped moulding compound, nozzle 11.

The relatively short fiber length associated with the material of 1/2 - inch squares apparently has a degrading effect on the nozzle tensile strength and shear force resistance of the resulting char. It appears to be advantages to have the individual fibers firmly anchored within a portion of the virgin material for as long as period of time during the run as possible. Rosette Layup with and without additives- Nozzles 1, 2, 3, and 4 were tested to compare the relative erosion resistance of a rosette type layup. Erosion data for all four nozzles are presented.

Nozzle 1 contained a chromium salt, which was added to the large diameter cloth material prior to impregnation. The overall erosion rate, after 250 seconds run time, was calculated at 1.280 mils per second(0.0325mm/sec).

Nozzle 2 again contained the chromium –salt additive to the large – diameter cloth, but, in this case , the coated cloth material was subjected to an additional proprietary procece which converted the cloth-salt combination to a more refractory –type reinforcement. An improvement in the overall erosion resistance over nozzle 1 was obtained and was calculated to be 0.930 mil per second (0.0236mm/sec).

Since previous testing had indicated that smaller-diameter cloth might be superior in erosion resistance to larger resistance to larger – diameter cloth material, an attempt was made to procure a third nozzle which was identical to nozzle 2, except that the small-diameter cloth material would be used. Unfortunately, this nozzle configuration did not prove possible as the mall-diameter cloth material lost approximately 80 percent of its physical strength during the proprietary conversion process.

Since a chemical analysis was not performed on both the nozzles 3 can only be evaluated on the basis of its initial constituents A relatively high erosion rate of 1.280 mils per second (0.0325mm/sec) A relatively high erosion rate of 1.280 mils per second(0.0325mm/sec) would indicate no particular advantage from this alternate material. The potential advantages of the chromium-salt conversion process (as shown by the comparative erosion rates of nozzles 1 and 2) may prove promising, especially if a method is found to treat the small diameter cloth, although are full attention to processing variables would be required.

Nozzle 4 was made from small-diameter cloth and contained no chromium-salt additive. The overall erosion rate was the lowest of any composite and also affords a direct path of the gases to escape. Since it is desirable to maximize the heat absorbed by endothermic reactions (formation of refractory SiC, graphites, etc.) between the gases and the reinforcing matrix, the dwell time of the gases becomes an important parameter. Increasing the dwell time and hopefully absorbing more energy could be accomplished by reducing the orientation angle of the unidirectional material from 90 degrees to some lower value. A possible further increase in the veer all erosion resistance of nozzle 6 may be expected. This procedure would be particularly applicable to long firing durations.

High and low resin content: The unidirectional fabric was chosen to assess the gross effect of resin concentration on erosion rate. Figure 14 compares the erosion resistance of a 22-percent resin content material (nozzle 6) to a material containing 35-percent resin (nozzle 7). Although nozzle 7 experienced the same effective radius change for the first 100 seconds, nozzle 6 was superior for the remainder of the run and had a greater overall resistance erosion. The excess resin of nozzle 7 compared to nozzle 6 additional cooling capacity during the early portion of the run. For longer firing durations, however, the reduced reinforcement content proved detrimental. The magnitude and duration of both curves under the zero erosion line indicates the relative ease by which the decomposed resin gases are able to enter the boundary layer for he unidirectional fibers.

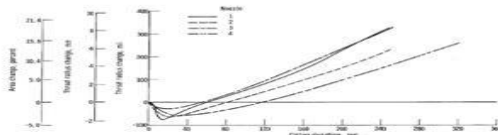


Figure 11. A typical case for nozzle 1, 2, 3, 4, 5, 6, 7, 8, 9, 10, 11, 12, 13, 14, 15, 16, 17, 18, 19, 20, 21, 22, 23, 24, 25, 26, 27, 28, 29, 30, 31, 32, 33, 34, 35, 36, 37, 38, 39, 40, 41, 42, 43, 44, 45, 46, 47, 48, 49, 50, 51, 52, 53, 54, 55, 56, 57, 58, 59, 60, 61, 62, 63, 64, 65, 66, 67, 68, 69, 70, 71, 72, 73, 74, 75, 76, 77, 78, 79, 80, 81, 82, 83, 84, 85, 86, 87, 88, 89, 90, 91, 92, 93, 94, 95, 96, 97, 98, 99, 100.

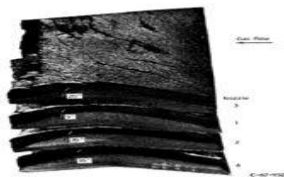
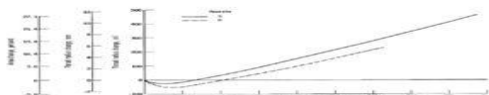


Figure 12. Comparison of nozzle 6 and nozzle 7 throat area.



E. Best And Lead Erosion-Resistant Materials Studied

Nozzle 4 represents the accumulative effect on the erosion resistance when many of the variables, previously exposed individually, are incorporated into the nozzle. The results may be considered an approach to optimization. Nozzle 4 which had the greatest resistance to erosion, is plotted on figure 15 together with the data for nozzle 9, which demonstrated the least resistance to erosion. The extended time (117sec) for nozzle 4 to experience positive erosion is caused primarily by the evolution of decomposition products of the resin binder into the boundary layer. the relatively rapid initiation of positive erosion for nozzle 9 was due to the very low percentage resin binder(13 percent) in addition, the silicon resin copolymer results in a very small percentage of gaseous decomposition products available for cooling purposes during steady operating, the small-diameter cloth, high-char density and rosette layup all contributed to the greater erosion resistance of nozzle 4, while the lower erosion resistance of nozzle 9 was apparently a function of the low shear force resistance of the elastomeric additive(25 percent). A significant effect on the erosion rate may also be seen.

After 140 seconds of normal running on nozzle 9, the injector became unstable the rapid increase in the erosion rate for the last 10 seconds of operation was quite pronounced. The frequency of the instability was measured at 2200 cycles per seconds(2200HZ) a subsequent (stable) run on nozzle 9, from 150 t0 250 seconds, made with the same injector, resulted in an operation rate equivalent to the first run prior to the instability.

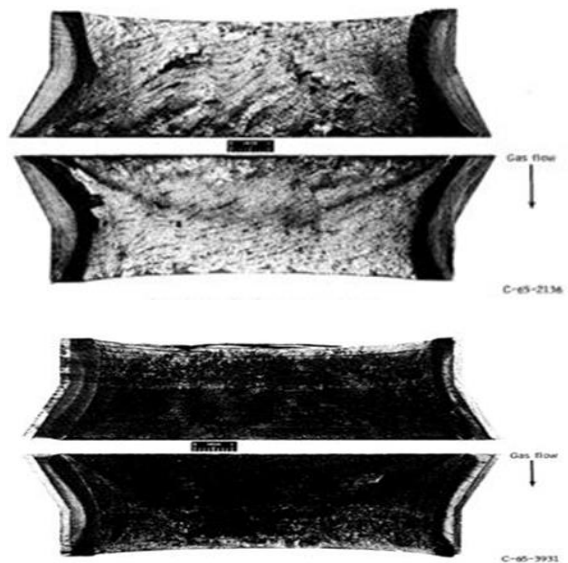
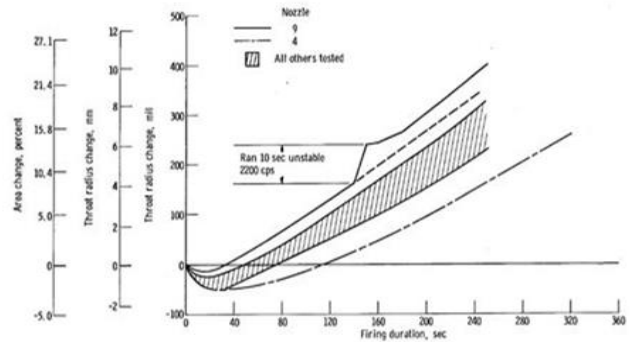


TABLE II - TEST RESULTS

Nozzle	Throat diameter				Erosion rate after 250-sec run		Area change after 250-sec run		Char to insulation		Condition of throat after firing	Nozzle desc
	Initial		After 250-sec run		mil/sec	cm/sec	Percent	Percent	After run of - sec			
	in.	cm	in.	cm								
4	7.818	19.83	8.137	20.67	0.6383	1.632	8.34	62	105	Minor gouging, moderate delamination, spallation in char	Small diameter, 1	
8	7.831	19.89	8.200	21.02	.932	2.368	12.25	---	---	-----	Small diameter, 1 low resin	
2	7.828	19.87	8.295	21.03	.93415	2.372	12.25	60	150	Minor gouging, moderate delamination, spallation in char	Large diameter, 1 rosette	
10	7.8298	19.88	8.6040	21.35	1.060	2.690	13.90	100	150	Minor gouging, char to outside diameter, slight delamination	Large diameter, 1 powder filled	
6	7.829	19.88	8.402	21.35	1.150	2.930	15.22	---	---	-----	Small diameter, 1	
7	7.811	19.80	8.284	21.30	1.110	2.920	15.22	65	150	Minor gouging, moderate cracking and delamination	Small diameter, 1 high resin	
11	7.8260	19.88	8.407	21.35	1.158	2.940	15.33	70	250	Minor gouging, minor cracks in char	Large diameter, 1 squares, fine si	
9	7.823	19.85	8.4348	21.46	1.265	3.265	15.98	100	150	Minor gouging, char to outside diameter, severe delamination	Large diameter, 1	
1	7.826	19.86	8.462	21.47	1.273	3.230	16.93	88	200	Minor gouging, moderate delamination, spallation in char	Large diameter, 1	
3	7.825	19.86	8.4819	21.55	1.274	3.238	17.59	60	200	Minor gouging, moderate delamination, spallation in char	Small diameter, 1 modified resin	
9	7.822	19.85	8.632	21.92	1.635	4.155	21.48	82	250	Minor gouging, minor delamination	Large diameter, 1 phenyl silane	

VIII. CONCLUSIONS

An investigation was conducted to evaluate 11 high-purity-silica reinforced ablative material samples as nozzles sections of a storable propellant nitrogen tetroxide (N2O4 and a 50-50 blend of unsymmetrical di-methyl-hydrazine UDMH with hydrazine N2H4) rocket engine testing was performed at an oxidant-to-fuel ratio of 2.0 a chamber pressure of 100psia (689kN/m2), and a nominal throat diameter of 7.82 inches (19.8 cm)

1. Light weight (small fibre diameter) high-purity-silica cloth had slightly higher erosion resistance than metals & non-metals.
2. The most erosion-resistant material of those tested was a lightweight high-purity-silica cloth materialism Preimpregnated with 27% polyamide Phenolic resin, layer up in a 35 degrees rosette pattern with no additive to the cloth material.
3. The least erosion resistant material tested was a heavy weight high-purity-silica cloth impregnated with 25% elastomer and 13 percent phenyls lane resin with fibres oriented 90 degrees to the nozzle centreline.
4. Finally it was found that “**ablative composite materials**” are appropriate for De-Laval rocket nozzle.

REFERENCES

1. Salmi, Reino J.; Wong, Alfred; and Rollbuhler, Ralph J.: *Experimental Evaluation of Various Non-metallic Ablative Materials as Nozzle Sections of Hydrogen-Oxygen Rocket Engine*. NASA TN D-3258, 1966.
2. Peterson, Donald A.; and Meyer, Carl L.: *Experimental Evaluation of Several Ablative Materials as Nozzle Sections of a Storable -Propellant Rocket Engine*. NASA TM X -1223, 1996.
3. Shinn, Arthur: *Experimental evaluation of six ablative material thrust chambers as components of storable propellant rocket engines*. NASA TN D-3945, 1967.
4. Hall, William B.: “*Standardization of the Carbon-Phenolic Materials and Processes, Volume I, Experimental Studies,*” Professor of Chemical Engineering, Mississippi State University, August 31, 1988.
5. Kelly, P. and Thompson, A.: “*AIAA 89-2661 Low Density Indications in Radiographs of Solid Rocket Motor Ablatives,*” 25th Joint Propulsion Conference, Morton Thiokol Inc., July 10-12, 1989.
6. TWR-10341 (CD) Rev. D: “*Manufacturing Plan for Space Shuttle Redesigned Solid Rocket Motor Project,*” Prepared by Morton Thiokol Inc., Manufacturing Engineering, NASA Contract NAS8- 30490.

